JOURNAL OF NATURAL PRODUCTS

pubs.acs.org/jnp

Article

Isolation, Identification, and Decomposition of Antibacterial Dialkylresorcinols from a Chinese *Pseudomonas aurantiaca* Strain

Yue Shi, Diana A. Zaleta-Pinet, and Benjamin R. Clark*

Cite This: https://dx.doi.org/10.1021/acs.jnatprod.9b00315

Read Online

ACCESS | Metrics & More | Article Recommendations | Supporting Information

ABSTRACT: A chemical investigation of a Chinese *Pseudomonas aurantiaca* strain has yielded a new benzoquinone (**4**) and furanone (**5**), in addition to the known dialkylresorcinols **1** and **2**. Extensive decomposition studies on the major metabolite **1** produced an additional furanone derivative (**6**), a hydroxyquinone (**7**), and two unusual resorcinol and hydroxyquinone dimers (**8** and **9**). Structures were elucidated by nuclear magnetic resonance spectroscopy in combination with tandem mass spectrometry analysis. These studies illustrate the potential of artifacts as a source of additional chemical diversity. Compounds **1** and **2** showed moderate antibacterial activity against a panel of Gram-positive pathogens, while the antibacterial activities of the artifacts (**4**–**9**) were reduced.

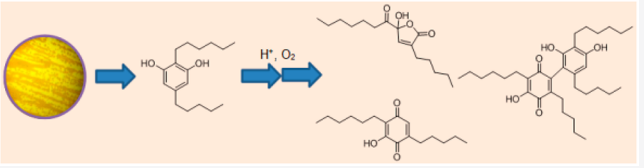

With the widespread use of antibiotics, drug-resistant bacteria have become increasingly prevalent and some infectious pathogens have developed resistance to most commonly available antibiotics, which increases the chance of treatment failure.[1] Microbial natural products are structurally diverse and can serve as a source of novel molecular scaffolds for drug development, especially in the field of antibiotic discovery.[2] In addition, metagenomic sequencing of environmental samples has revealed that the majority of microbial biodiversity has yet to be chemically explored, often as a result of the difficulty of growing many species under laboratory conditions.[3] China, a country with a large territory and highly varied climate, offers significant potential for microbial natural product discovery,[4−6] to discover novel antibiotics that can meet the resistance challenge.[7,8]

Pseudomonas is a genus of Gram-negative bacteria commonly acting as rhizosphere colonizers. They have been reported to produce more than 100 antibacterial compounds,[9] including lipopeptides,[10] lipodepsipeptides,[11] diketopiperazines,[12] rhamnolipids,[13] pseudotrienic acids,[14] and dialkylresorcinols.[15] One of the characteristic metabolite classes produced by the *Pseudomonas* genus are the dialkylresorcinols, which have displayed antimicrobial activity against Gram-positive bacteria, mycobacteria, yeasts, and filamentous fungi.[16,17] A great number of dialkylresorcinol derivatives have been described from *Pseudomonas* and related genera.[14−20] Biosynthetic studies using isotopic labeling strategies have delineated the biosynthetic pathway, an unusual head-to-head condensation of two medium-chain-length fatty acid precursors.[21]

The current report describes the chemical investigation of a Chinese isolate of *Pseudomonas aurantiaca*. In addition to describing the isolation and structure elucidation of secondary metabolites, a study of the decomposition of its major products, the dialkylresorcinols, was carried out. On the basis of detailed chemical analysis of the decomposition of the dialkylresorcinol **1** under acidic and basic conditions, four new products were elucidated, including two dimers. This report differentiates the natural and artificial products produced during the culture and isolation process, by demonstrating transformation from dialkylresorcinols into mono- and dimeric derivatives.

RESULTS AND DISCUSSION

The bacterium YM03-Y3 was isolated from a soil sample collected in the Yellow Mountains, Anhui Province, China, and was identified as *P. aurantiaca* by 16S rDNA sequencing.[22] The methanol extract of YM03-Y3 was analyzed by high-performance liquid chromatography (HPLC) (Figure S2 of the Supporting Information), showing numerous high-intensity peaks, indicating the presence of diverse secondary metabolites. In addition, the extract also presented significant biological activity against a panel of microbial pathogens (Figure S1 of the Supporting Information), suggesting that it was a suitable candidate for further investigation. Culture conditions of YM03-Y3 were optimized by the selection of an appropriate medium, pH, and temperature to maximize metabolite production. Fractionation of a large-scale culture led to the isolation of five compounds **1**−**5**, of which the structures (Figure 1) were elucidated by detailed spectroscopic analysis.

Received: April 5, 2019

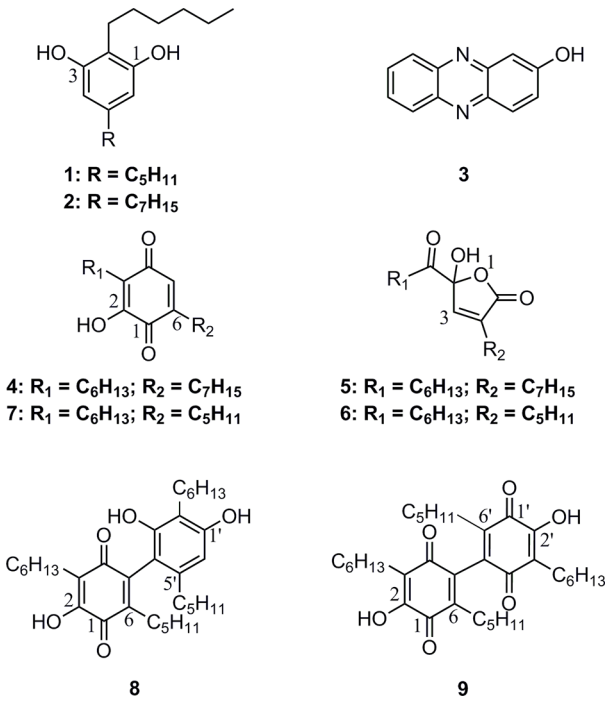

Figure 1. Natural products and artifacts isolated from *P. aurantiaca* (YM03-Y3). All alkyl chains are linear.

Compounds **1** and **2** have been previously reported as natural products from *Pseudomonas* sp. Ki19.[15,16] Experimental ^{1}H and ^{13}C nuclear magnetic resonance (NMR) and high-resolution mass spectrometry (HRMS) data corresponded well with previously reported literature data (Table 2 and Table S1 of the Supporting Information). To further characterize these molecules, high-resolution tandem mass spectrometry ($HRMS^2$) was conducted (Figures S3 and S4 of the Supporting Information), revealing fragments at m/z 195.1378 ($C_{12}H_{19}O_2$, calculated for 195.1380) and m/z 181.1219 ($C_{11}H_{17}O_2$, calculated for 181.1223) corresponding to losses of C_5H_{10} and C_6H_{12} in compound **1**, while m/z 209.1530 ($C_{13}H_{21}O_2$, calculated for 209.1536) and m/z 195.1378 ($C_{12}H_{19}O_2$, calculated for 195.1380) corresponded to losses of C_6H_{12} and C_7H_{14} in compound **2**. The intensity of fragments resulting from the loss of the alkyl chains at C-2 was significantly stronger than that resulting from the loss of the C-5 alkyl chain. Compound **3** was structurally unrelated to the other compounds in the extract and was identified as 2-hydroxyphenazine by comparison of high-resolution electrospray ionization mass spectrometry (HRESIMS) and ^{1}H NMR spectra to reported data (Table S1 of the Supporting Information).[12]

Compound **4** was isolated as a yellow pigment. The ultraviolet (UV) spectrum suggested that it possessed a typical benzoquinone chromophore with absorption maxima at 210, 270, and 390 nm. ^{13}C and heteronuclear multiple-bond correlation (HMBC) NMR revealed 6 downfield resonances, including 2 carbonyl signals at 185.2 and 190.0, in addition to 13 resonances consistent with aliphatic carbons (Table 1). A comparison of the proton and carbon NMR to literature data[15] made it clear that compound **4** was an homologue of the known compound, 2-hexyl-3-hydroxy-5-pentylbenzo-1,4-quinone[15] (**7**), with the addition of two additional methylene groups, which was supported by HRESIMS (measured 305.2126, $[M - H]^-$, $C_{17}H_{30}O_3$, calculated for 305.2122). HMBC data showed correlations from the two downfield methylene signals (δ_H 2.39 and 23.7) (Figure 2) to carbons at δ_C 185.2 and 190.0, respectively, indicating the presence of two carbonyl groups, consistent with a dialkyl-substituted hydroxybenzoquinone. Correlation spectroscopy (COSY) experiments showed a cross peak between 6.40 ppm (H5) and 2.39 ppm (H6a), resulting from a weak four-bond coupling. The known dialkylhydroxyquinone **7** has been reported as an oxidation product from compound **1**; both possess *n*-hexyl and *n*-pentyl substituents.[15] On the basis of a comparison to literature data, the alkyl groups were assigned as shown for

Table 1. NMR Spectroscopic Data for Compounds 4−6 (d_4-MeOH, 400 MHz)

compound **4**			compound **5**			compound **6**	
number	δ_C	δ_H, mult	number	δ_C	δ_H, mult (J in Hz)	δ_C	δ_H, mult (J in Hz)
1	185.0						
2	155.1		2	105.9[a]		104.9[a]	
3	122.1		3	145.7[a]	7.00, s	145.6	6.99, s
4	189.8		4	139.4[a]		139.3	
5	134.5	6.41, s	5	173.1		173.6	
6	147.0		2a	204.4		204.6	
3a	23.2	2.37, m	2b	37.5	2.62, t (7.0)	37.5	2.63, t (7.2)
3b	30.1	1.44, m	2c	24.3	1.55 m	24.3	1.56, m
3c	32.9	1.35, m	2d	30.1	1.36, m	29.8	1.36, m
3d	30.4	1.31, m	2e	32.7	1.29, m	32.4	1.30, m
3e	23.7	1.31, m	2f	23.6	1.29, m	23.4	1.30, m
3f	14.4	0.89, m	2g	14.4	0.90, m	14.3	0.91, m
6a	29.4	2.39, m	4a	26.2	2.31, t (7.5)	26.1	2.30, t (7.6)
6b	29.0	1.52, m	4b	28.4	1.57, m	28.1	1.58, m
6c	32.8	1.35, m	4c	30.2	1.36, m	32.7	1.36, m
6d	30.4	1.31, m	4d	29.8	1.29, m	23.6	1.30, m
6e	29.2	1.31, m	4e	32.7	1.29, m	14.3	0.91, m
6f	23.7	1.31, m	4f	23.7	1.29, m		
6g	14.4	0.89, m	4g	14.4	0.90, m		

[a]Indicated carbon shifts were obtained from the HMBC spectrum.

https://dx.doi.org/10.1021/acs.jnatprod.9b00315
J. Nat. Prod. XXXX, XXX, XXX−XXX

Table 2. NMR Spectroscopic Data for Compounds 1 and 7−9 (d_4-MeOH, 400 MHz)

compound 1			compound 7			compound 8, fragment A			compound 8, fragment B			compound 9		
number	δ_C	δ_H, mult[a]	number	δ_C	δ_H, mult	number	δ_C	δ_H, mult	number	δ_C	δ_H, mult	number	δ_C	δ_H, mult
1	157.0		1	184.9		1	185.2		1′	157.1		1/1′	183.2	
2	114.6		2	155.1		2	154.4		2′	115.2		2/2′	151.0	
3	157.0		3	122.1		3	122.5		3′	153.6		3/3′	121.8	
4	107.8	6.13, s	4	189.8		4	189.5		4′	113.8		4/4′	185.7	
5	142.2		5	134.5	6.41, s	5	144.3		5′	139.7		5/5′	139.7	
6	107.8	6.13, s	6	147.0		6	145.4		6′	108.3	6.30, s	6/6′	142.4	
2a	24.0	2.54, t (7.2)	3a	23.4	2.38, m	3a	23.5	2.44, m	2′a	23.8	2.59, m	3a/3′a	23.0	2.42, m
2b	30.3	1.49, m	3b	29.4	1.44, m	3b	30.3	1.47, m	2′b	29.4	1.47, m	3b/3′b	28.3	1.44, m
2c	33.1	1.31, m	3c	32.8	1.35, m	3c	29.8	1.37, m	2′c	33.2	1.31, m	3c/3′c	29.5	1.26, m
2d	32.7	1.31, m	3d	30.4	1.31, m	3d	33.0	1.14, m	2′d	32.9	1.31, m	3d/3′d	32.1	1.26, m
2e	23.6	1.31, m	3e	23.4	1.31, m	3e	23.2	1.14, m	2′e	24.1	1.31, m	3e/3′e	22.4	1.26, m
2f	14.4	0.90, m	3f	14.4	0.92, m	3f	14.5	0.78, m	2′f	14.4	0.87, m	3f/3′f	14.4	0.82, m
5a	36.7	2.39, t (7.2)	6a	29.3	2.40, m	6a	30.0	2.23, m	5′a	34.7	2.13, m	6a/6′a	28.2	2.31, m
								2.12, m						2.07, m
5b	32.2	1.56, m	6b	28.8	1.54, m	6b	28.8	1.37, m	5′b	31.3	1.31, m	6b/6′b	28.1	1.26, m
5c	30.6	1.31, m	6c	32.6	1.35, m	6c	33.2	1.22, m	5′c	30.4	1.31, m	6c/6′c	31.7	1.26, m
														1.21, m
5d	23.8	1.31, m	6d	23.6	1.31, m	6d	28.6	1.22, m	5′d	23.7	1.31, m	6d/6′d	22.7	1.21, m
5e	14.5	0.90, m	6e	14.3	0.92, m	6e	14.4	0.87, m	5′e	14.2	0.87, m	6e/6′e	14.2	0.86, m

[a]Coupling constants in hertz.

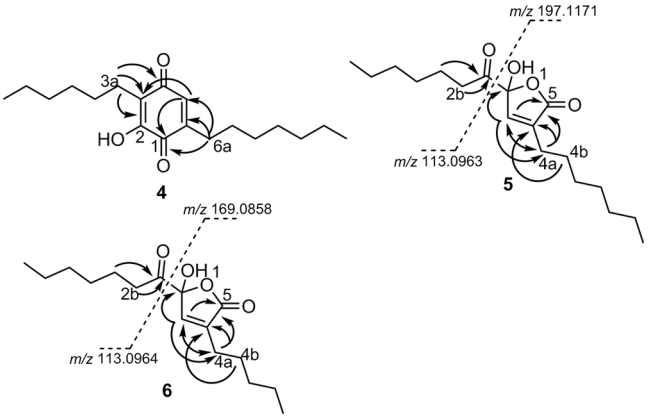

Figure 2. Key HMBC (H → C) correlations and MS−MS fragments for compounds 4−6.

compound 4. It is plausible that compound 4 might be formed by an analogous oxidation of compound 2.

Compound 5 was obtained as a white solid and showed ultraviolet/visible (UV/vis) absorption maxima at 200, 220, and 280 nm. Its molecular formula was determined to be $C_{18}H_{30}O_4$ by HRESIMS, indicating 4 degrees of unsaturation. The ^{13}C NMR spectrum revealed the presence of 13 aliphatic carbon signals between 14.4 and 37.6 ppm, including two methyl carbons. In addition to two downfield methylene ^1H NMR signals at 2.63 and 2.30 ppm, this suggested the presence of two linear aliphatic chains in the structure. The carbon signals in the HMBC spectrum (Figure 2) revealed the presence of five distinct downfield carbons, one sp^3 carbon at 105.9 ppm, two alkene carbons at 139.4 and 145.7 ppm, and two carbonyl groups: one at 204.4 ppm, which suggested a non-conjugated ketone, and another at 173.1 ppm, suggesting the presence of an ester. The furanone core was established with the HMBC spectrum, with the olefinic proton at 7.00 ppm showing four cross peaks to three sp^2 carbon signals at 105.9 ppm (C2), 139.4 ppm (C4), 173.1 ppm (C5) and to one aliphatic carbon at 26.1 ppm, which was assigned as C4a. The attached methylene protons H4a, in turn, showed HMBC correlations to C3, C4, and C5, while H4b correlated to C4, confirming the location of one of the aliphatic chains at C4. For the other chain, the HMBC correlations observed from two methylene protons H2b at 2.61 ppm and H2c at 1.55 ppm to C2a (204.1 ppm), indicating that carbonyl carbon was attached to the second alkyl chain. The only remaining position to link the two major fragments was to connect C2a to carbon 2; however, the high chemical shift of C2 and lack of any directly attached protons suggested that it was further substituted and that the remaining hydroxy group was located at this position. As previously established, NMR signals evidenced the presence of 13 aliphatic carbons (Table 1), but as a result of the lack of HMBC correlation from H2c/C4b to a methyl carbon, it was impossible to establish the length of the individual aliphatic chains using NMR data alone.

To determinate the specific number of carbons in each chain, ESIMS[2] analysis was employed (Figure S5 of the Supporting Information). The tandem mass spectrometry (MS−MS) spectrum resulting from fragmentation of the protonated molecule at m/z 311.2213 $[M + H]^+$ revealed a fragment at m/z 197.1171 ($C_{11}H_{17}O_3$, calculated for 197.1172), consistent with cleavage between C2 and C2a and consequent loss of $C_7H_{13}O$, while a strong signal at m/z 113.0963 ($C_7H_{13}O$, calculated for 113.0961) further supported this hypothesis. They both indicted that the aliphatic chain at position 2a was a *n*-hexyl chain; hence, the other alkyl chain attached at C4 should be a *n*-pentyl chain. Thus, the structure of compound 5 was assigned as shown in Figure 1. Circular dichroism (CD) analysis of compound 5 did not reveal any significant absorbances; this was attributed to the likely presence of a racemic mixture, as detailed further below.

Previous reports described that a solution of compound 1 could turn from colorless to pale yellow when allowed to stand in deuterated $CDCl_3$ in an NMR tube for 2 days;[15,16] a similar observation was noted in this study. However, only one oxidation product from compound 1 has been reported; the dialkylhydroxyquinone 7 mentioned above.[15] This change is

https://dx.doi.org/10.1021/acs.jnatprod.9b00315
J. Nat. Prod. XXXX, XXX, XXX−XXX

caused by a two-step oxidation mechanism, previously proposed by Singh et al.,[23] coupled with a similar degradation pathway reported by Philipp and Schink.[24]

Considering the structures of compounds **4** and **5** and the reports from previous research, it seemed possible that these compounds might also be artifact products from decomposition of compound **2**. As a preliminary experiment, a small amount of compound **1** (3 mg) was dissolved in chloroform (1.5 mL) and allowed to stand at room temperature; the decomposition process was monitored by HPLC. After 7 days, three additional major peaks could be observed in the HPLC chromatogram of the decomposition mixture (Figure 3a).

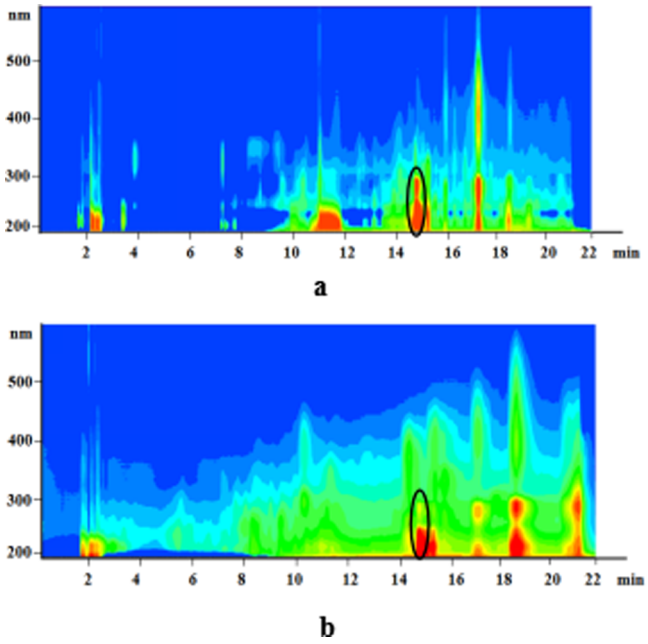

Figure 3. HPLC isoplot spectrum from 190 to 600 nm for a 7 day decomposition study of compound **1** (shown in black circles): (a) artifacts produced after decomposition in $CHCl_3$ and (b) artifacts produced after decomposition in NaOH−MeOH.

Artifacts can often be a fortuitous route for the discovery of new structures or stronger bioactivities.[25−27] Hence, a larger scale study (50 mg) with compound **1** was performed to further explore the decomposition products.

Decomposition of the compound was conducted in the same manner and yielded three major compounds: compounds **6** (2.4 mg), **7** (3.0 mg), and **8** (4.5 mg). Compound **7** possessed very similar NMR data to compound **4** and was rapidly identified as a known dialkylhydroxyquinone, with all spectroscopic data consistent with literature values.[15] However, compounds **6** and **8** were previously unreported molecules.

A comparison of NMR data and molecular formulas obtained from HRESIMS (305.1720, $[M + Na]^+$, $C_{16}H_{26}O_4$) led to the identification of compound **6** as a homologue of compound **5**, with the loss of two methylene units. HMBCs (Figure 2) as well as ^{13}C NMR data were almost identical to those of compound **5**, with only minor changes to shifts of alkyl carbons. However, one characteristic difference was observed, with a change in the chemical shift of C4a to 32.7 ppm (cf. 30.2 ppm in compound **5**). This indicated that the C4 alkyl chain had changed in length, while the C2 alkanone chain was unchanged, providing further evidence for the assigned structures of both compounds. Additional evidence was provided by MS−MS data (Figure S6 of the Supporting Information), which revealed MS^2 fragments, m/z 169.0858 ($C_9H_{13}O_3$, calculated for 169.0859) and m/z 113.0964 ($C_7H_{13}O$, calculated for 113.0961), analogous to those observed for compound **5**, which further supported the assignment of the structure for compound **6** as shown. Again, CD analysis did not reveal any significant absorbances, which suggests the presence of a racemic mixture. Given the artifactual nature of this compound and its likely formation through an achiral chemical process, this is not surprising.

The dialkylresorcinol−quinone dimer (**8**) was isolated as a red powder. The UV spectrum of compound **8** revealed absorption maxima at 230, 275, 375, and up to 490 nm. HRESIMS data were consistent with a molecular formula of $C_{34}H_{52}O_5$. The proton NMR resonances of compound **8** consisted of one aromatic singlet (6.30 ppm), three deshielded 2H methylenes (2.59, 2.44, and 2.13 ppm), one methylene unit with non-equivalent protons (2.23 and 2.12 ppm), four methyl groups [0.87 (3×) and 0.78 ppm], and numerous methylene groups around 1.30 ppm. The ^{13}C NMR spectrum revealed the presence of 12 carbons in the aromatic region: 189.5, 185.2, 157.1, 154.4, 153.5, 145.3, 144.3, 139.7, 122.5, 115.1, 113.2, and 108.2 ppm. Taken together and compared to the NMR data of compounds **1** and **7** suggested that compound **8** might be a dimer of these two fragments. Carbon signals at 185.2, 154.4, 122.5, 189.5, 144.3, and 145.3 ppm were assigned as part of hydroxyquinone (fragment A in Figure 4), while 157.1, 115.1, 153.5, 113.2, 139.7, and 108.2 ppm were attributed to a dialkylresorcinol (fragment B in Figure 4).

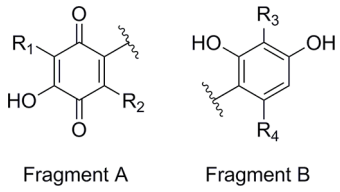

Figure 4. Substructures of compound **8**.

The HMBC data associated with substructure A indicated that there were correlations from a deshielded methylene proton at δ_H 2.44 (3a), correlating with carbon signals at 189.5 ppm (C4), 154.4 ppm (C2), and 122.5 ppm (C3), while a pair of diasterotopic methylene protons at δ_H 2.23 and 2.12 (6a) correlated with carbons at 185.2 ppm (C1) and 144.3 ppm (C5). Crucially, the aromatic singlet of **7** was absent from the spectrum. A suite of COSY correlations of mutually coupled methylenes together with ^{13}C NMR chemical shifts of numerous signals between 14.4 and 32.9 ppm and a number of deshielded methylenes confirmed the existence of two aliphatic chains and established the partial structure as substructure A.

HMBC signals associated with substructure B were similar to the known dialkylresorcinols, except for the lack of one aromatic proton at 6.13 ppm. There was a single aromatic singlet (δ_H 6.30) correlated with 157.1 (C1′), 115.1 (C2′), and 34.7 (C5′a) and two deshielded methylenes (H2′a and 5′a): 2′a correlated with carbons at 157.1 ppm (C1′), 153.5 ppm (C3′), and 115.1 ppm C2′), while H5′a correlated with carbons at 139.7 ppm (C5′), 113.2 ppm (C4′), and 108.2 ppm (C6′), respectively. Substructures A and B account for all ^1H and ^{13}C NMR signals observed in the NMR spectrum, and they are consistent with the assigned structure, in which the

https://dx.doi.org/10.1021/acs.jnatprod.9b00315
J. Nat. Prod. XXXX, XXX, XXX−XXX

Scheme 1. Inferred Decomposition Process of Compound 1, Including Proposed Minor Decomposition Products[a]

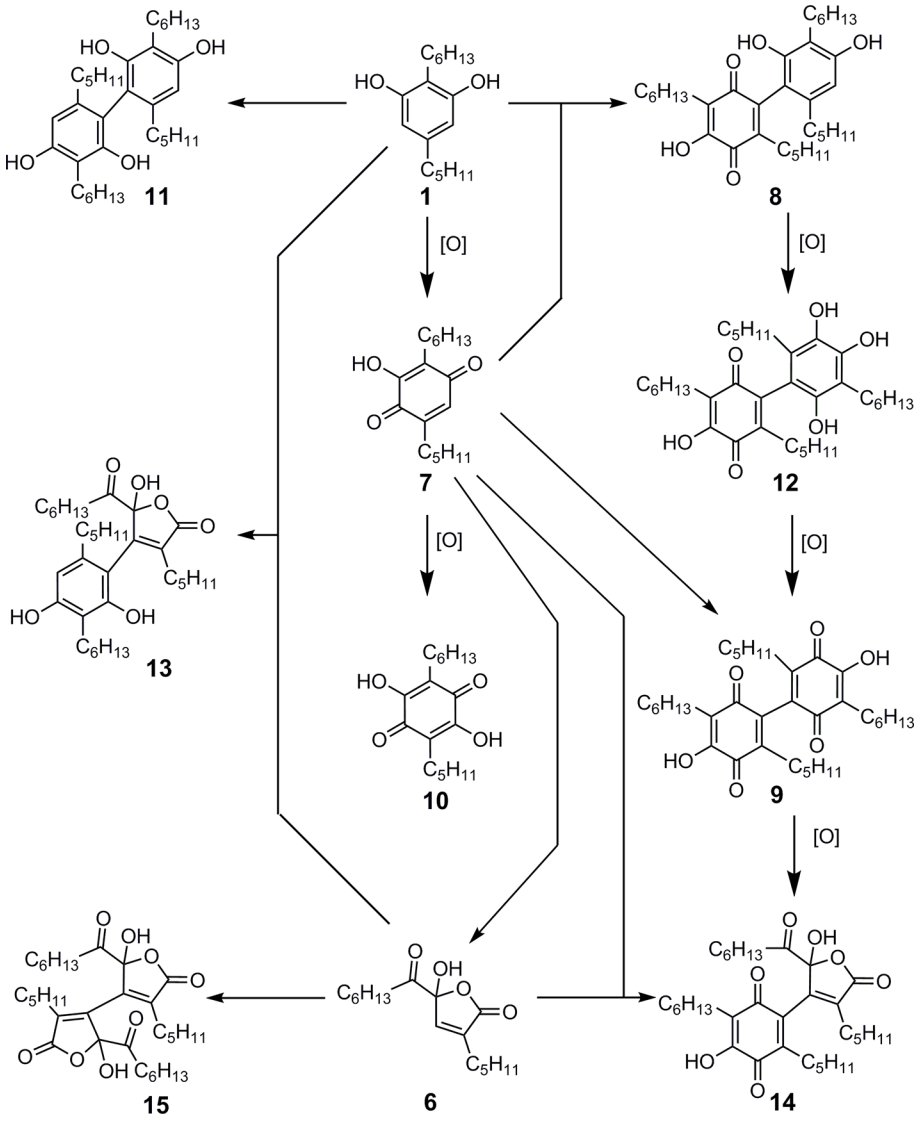

[a]Structures of compounds **10**–**15** are tentative and based on HRMS data. All alkyl chains are linear.

two fragments were directly linked from C5 to C4′. Under these circumstances, a chiral axis may exist along this bond, which could explain the presence of two non-equivalent methylene protons (H6) at 2.23 and 2.12 ppm.

Similar to compound **5**, the number of carbons in the C4 aliphatic chain was confirmed by HRESIMS^2 (Figure S7 of the Supporting Information). Some of these fragments were consistent with the fragmentation of the dimer into its two principal halves: m/z 265.2159 and 277.1795, which corresponded to the dialkylresorcinol and hydroxybenzoquinone portions of the molecule, respectively. In addition, fragments at m/z 457.2945 and 471.3107 corresponded to losses of C_5H_{10} and C_6H_{12}, similar to those observed for the monomeric dialkylresorcinol **1**. The remainder of the fragmentation was more complex; however, identities for some of the major fragments have been proposed (Scheme S1 and Table S12 of the Supporting Information). In combination, all spectral data were consistent with the structure shown (**8**). Compound **8** might be formed by a two-step reaction: first dialkylresorcinol **1** is oxidized into hydroxyquinone **7** via atmospheric oxidation under acid catalysis, which is then oxidatively dimerized with a second molecule of compound **1** to yield the heterodimer **8**.

Acid- and base-catalyzed decompositions can often yield dramatically different suites of compounds.[27] Thus, the decomposition procedure for compound **1** was repeated under basic conditions, using NaOH–MeOH (pH 10) as the solvent, which formed a pale purple solution over 7 days. HPLC monitoring of a small-scale decomposition mixture (Figure 3B) revealed products with retention times similar to those formed during the acid decomposition, with one exception, an intense peak at 21.2 min.

A larger scale experiment (50 mg of compound **1**) was carried out in aqueous methanol adjusted to pH 10 with NaOH, stirring at room temperature for 10 days. Isolation of the decomposition products was carried out using semi-preparative HPLC. Isolation resulted in compounds **6**–**8**, previously obtained in the acid decomposition, in addition to one new dimer (compound **9**, 5.1 mg). The different colors observed in acid and base decompositions are likely due to deprotonation of the hydroxyquinones; bathychromic shifts are common for phenolic compounds under basic conditions.[28]

https://dx.doi.org/10.1021/acs.jnatprod.9b00315
J. Nat. Prod. XXXX, XXX, XXX–XXX

Table 3. Minimum Inhibitory Concentration (MIC) (μg/mL) of Compounds 1−9 toward American Type Culture Collection (ATCC) Bacterial Pathogens

compound	*Staphylococcus aureus* ATCC 12600	*Staphylococcus epidermidis* ATCC 14990	*Enterococcus hirae* ATCC 8043	*Streptococcus mutans* ATCC 25175	*Bacillus subtillis* ATCC 6633
1	4.2	4.2	4.2	4.2	8.4
2	1.1	8.3	33.4	33.4	66.7
3	*a*	33.4	*a*	*a*	*a*
4	133	*a*	*a*	133	*a*
5	16.7	33.4	66.7	133	33.4
6	33.4	66.7	133	133	66.7
7	*a*	*a*	133	66.7	33.4
8	*a*	*a*	*a*	133	*a*
9	133	*a*	*a*	133	133
positive control[b]	0.26	0.52	1.1	1.1	1.1
negative control[c]	*a*	*a*	*a*	*a*	*a*

[a]No activity detected at tested concentrations. [b]See Table S7 of the Supporting Information for positive controls. [c]Distilled water was used as a negative control.

Compound **9** was isolated as a deep yellow solid. HRESIMS established the molecular formula as $C_{34}H_{50}O_6$. Carbon signals at 185.8 and 183.0 ppm, in addition to a characteristic UV/vis spectrum with maximum absorption at 230, 280, and 400 nm suggested a quinone substructure. There were 17 resonances in the ^{13}C NMR spectrum, and comparing this to the predicted molecular formula implied the presence of 2-fold symmetry in the molecule. Considering that this compound was derived from compound **1**, it was proposed that this might be a quinone dimer, with the same lengths of the alkyl chains as the monomeric quinone **7**. Ultimately, the structure of compound **9** is proposed as shown in Figure 1. Given the observation of two pairs of non-equivalent methylene protons (H6a and H6c and H6′a and H6′c), it suggested the presence of a chiral axis in the structure. HMBCs between methylene 3a (2.42 ppm) and C2−C4 (151.0, 121.8, and 185.8 ppm) and from H6a (2.31 and 2.07 ppm) to C1, C5, and C6 (183.0, 139.6, and 142.3 ppm) were also consistent with the proposed structure. Additional evidence obtained from HRESIMS^2 (Figure S8 of the Supporting Information) was the fragment at 277.1795 (calculated for $C_{17}H_{25}O_3$, 277.1798) corresponding to the monomeric fragment; major fragments are listed in Scheme S2 and Table S13 of the Supporting Information.

The structure of the major compounds identified in the decomposition study, compounds **6**−**9**, also suggested that compounds **4** and **5**, isolated during the initial isolation, could be artifacts as a result of changes in pH and exposure to oxygen during the culture and isolation process. It is assumed that decomposition of compound **2** would yield a similar suite of products to those derived from compound **1** but with *n*-heptyl in place of *n*-pentyl substitution, although this was not tested in this study.

In addition to the major products of the decomposition, several minor products were detected by liquid chromatography−mass spectrometry (LC−MS) under both acidic and basic conditions. We have tentatively proposed structures (compounds **10**−**15** in Scheme 1) based on the information obtained by HRESIMS and the already known decomposition outcomes (Table S14 of the Supporting Information). On the basis of the isolated decomposition products, dialkylresorcinol (**1**) could first be oxidized into the hydroxyquinones (**7** and **10**) and, subsequently, further oxidized and rearranged to give the furanones **6**, with the loss of one carbon unit. Subsequently, hydroxyquinone is dimerized with either dialkylresorcinol **8** or itself (**9**) through an aromatic coupling process. Compound **12** might be an intermediate product in the process of dimerization to form compound **9**. In a similar manner, hydroxyquinones, dialkylresorcinols, and furanones might also be dimerized to form either homodimers (**13** and **14**) or heterodimers (**11** and **15**) (Scheme 1).

All isolated compounds were screened against a panel of microorganisms (Table S7 of the Supporting Information). The results (Figure S1 of the Supporting Information) showed that compounds were active against Gram-positive bacteria. Compound **1** showed moderate activity (4−8 μg/mL) against all strains tested, while compound **2** displayed the strongest activity against *Staphylococcus aureus* (1.1 μg/mL); the decomposition products presented weaker biological activity compared to the parent compounds (Table 3).

Reasons for this loss of activity are uncertain; however, oxidation to quinones reduces the polarity of the substituents and may negatively affect their bioavailability. Likewise, the formation of dimers increases the molecular mass and may lead to a reduction in solubility. Little is known about the mode of action of the dialkylresorcinols; they are known to interact with the PauR receptor in *Photorhabdus asymbiotica* in quorum-sensing processes,[29] but the precise details of the interaction have not yet been delineated.

EXPERIMENTAL SECTION

General Experimental Procedures. Samples were dried in a Savant SC210A SpeedVac concentrator with VLP120 vacuum pump (Ameritech). HPLC and UV spectra were obtained on an Agilent spectrophotometer (Agilent 1260 Infinity). Semi-preparative HPLC purifications were performed on LC-20AR Series semi-preparative HPLC (Shimadzu, Japan) using a 5 μm Agilent ZORBAX SB-C_{18}, 9.4 × 250 mm column with a flow rate of 2.5 mL/min. ^1H and ^{13}C NMR spectra were recorded on a 400 or 600 MHz spectrometer (Bruker Avance III) at 25 °C. HRMS was obtained on a Q-TOF micro spectrometer (Agilent micrOTOF-Q II) and an ESI-Orbitrap spectrometer (Thermo Fisher Q Exactive HF). Electronic circular dichroism (ECD) spectra were measured on a Bio-Logic MOS-500 spectrometer using a 1 cm path length quartz cuvette at 2 nm slit size.

Microbial Material. The strain YM03-Y3 was isolated from soil collected in the Yellow Mountains (Huangshan), Anhui Province, China, on July 2, 2016. Soil was taken from the top of the mountain, approximately 1 m away from a river, during the raining season, at GPS coordinates 30° 08′ 25″ N, 118° 10′ 03″ E. The isolate was

https://dx.doi.org/10.1021/acs.jnatprod.9b00315
J. Nat. Prod. XXXX, XXX, XXX−XXX

identified as *P. aurantiaca* by sequence analysis of 16S rDNA; the sequence has been submitted to GenBank under accession number SUB5407677 Seq1 MK744062. It was cultured in Czapek−Dox medium and stored at −80 °C with glycerol. All strains used for antimicrobial activity assays in this study are ATCC pathogens (Table S7 of the Supporting Information).

Strain Identification. Purified samples of bacteria were used for DNA extractions. DNA isolation, amplification, and sequence analysis were carried out using an adaption of existing protocols (page S42 of the Supporting Information).[22]

Standard Analytical HPLC Method. Column, ZORBAX SB-C_{18}, 3.5 μm, 4.6 × 150 mm; flow rate, 0.8 mL/min; and gradient, 10% acetonitrile (ACN) in the first minutes, up to 100% ACN at 15 min, and retained at 100% ACN for 3 min before returning to original conditions for the next run.

Isolation and Purification. After 10 days of fermentation under optimized conditions (shaking under 200 rpm, at 30 °C, in a 2 L Erlenmeyer flask containing 1 L of Czapek−Dox broth, total 15 L broth), cell and supernatant fractions of the cultures were separated by centrifugation at 4000 rpm for 20 min. Supernatant was extracted by liquid−liquid extraction with ethyl acetate (22.5 L) and then *n*-butanol (22.5 L) to yield 902 mg and 1.35 g of crude extract, respectively. Biomass was separately extracted with methanol, yielding 600 mg of crude extract. All fractions possessed similar HPLC profiles and were combined and concentrated together in a SpeedVac prior to further separation. The combined extracts (2.85 g) were separated through on a HP20 resin column using a stepwise elution of methanol−water (200 mL of each gradient) and finally ethyl acetate to give four fractions (100% H_2O, 50% H_2O−MeOH, 100% MeOH, and 100% EtOAc). The 100% H_2O fraction contained largely large polarity metabolites and water-soluble medium components and other high-polarity metabolites and was not investigated further. The three remaining fractions were (1.97 g) recombined and fractionated using silica gel open column chromatography with a hexane−ethyl acetate gradient (step gradient: hexane−EtOAc of 20:1, 10:1, 5:1, 3:1, 2:1, 1:1, 1:3, 1:5, 1:10, and 1:20, 100% EtOAc, 100% EtOH, 150 mL of each gradient) to afford 10 fractions (F_1−F_{10}). The major fraction, F_3 (650 mg), was subjected to semi-preparative HPLC (linear gradient elution of 55:45−100:0 ACN−H_2O over 60 min and then kept at 100% ACN for 20 min) to yield dialkylresorcinol (**1**, t_R = 15.5 min with standard analytical HPLC gradient, 125 mg) and dialkylresorcinol (**2**, t_R = 16.5 min, 110 mg). The remaining material of fraction F_3 was further purified by another round of preparative HPLC (linear gradient elution of 65:35−85:15 ACN−H_2O over a period of 40 min, then gradient elution up to 100% ACN over 10 min, and kept at 100% ACN for 15) to give a new furanone derivative (**5**, t_R = 17.1 min, 2.4 mg). Fraction F_{10} (155 mg) was separated by semi-preparative HPLC using a linear gradient elution of 25:75−70:30 ACN−H_2O over 50 min to yield 2-hydroxyphenazine (**3**, t_R = 9.1 min, 3.5 mg). The deep red-colored fraction F_1 (420 mg) was fractionated using HPLC with an isocratic elution of 90% ACN−H_2O and yielded quinone (**4**, t_R = 19.3 min, 4.5 mg).

Large-Scale Decomposition Study. *Acid Decomposition.* Compound **1** (50 mg) was dissolved with 10 mL of chloroform and stirred at room temperature for 10 days. Purification of the resulting mixture was carried out using reversed-phase preparative HPLC (gradient elution from 55 to 90% ACN over 40 min), to yield compounds **6** (t_R = 15.6 min, 2.4 mg), **7** (t_R = 17.8 min, 3.0 mg), and **8** (t_R = 19.1 min, 4.5 mg).

Base Decomposition. Compound **1** (50 mg) was dissolved in methanol (20 mL), with the pH adjusted to 10 with 0.1 mol/L NaOH, and then stirred at room temperature for 10 days. Isolation of the decomposition products was performed using reversed-phase semi-preparative HPLC as described above to yield compounds **6**−**8** again and compound **9** (t_R = 21.2 min, 5.1 mg).

*2-Hexyl,5-pentyl-1,3-resorcinol (**1**):* White, amorphous powder; UV (MeOH) λ_{max}, 210, 270 nm; ^1H and ^{13}C NMR data, see Table 2; positive HRESIMS ion, *m*/*z* 265.2155 $[M + H]^+$ (calculated for $C_{17}H_{29}O_2$, 265.2162).

*2-Hexyl,5-heptyl-1,3-resorcinols (**2**):* White, amorphous powder; UV (MeOH) λ_{max}, 210, 270 nm; ^1H and ^{13}C NMR data, see Table S1 of the Supporting Information; positive HRESIMS ion, *m*/*z* 293.2468 $[M + H]^+$ (calculated for $C_{19}H_{33}O_2$, 293.2475).

*2-Hydroxyphenazine (**3**):* Orange, amorphous powder; UV (MeOH) λ_{max}, 210, 260, 350, 400 nm; ^1H and ^{13}C NMR data, see Table S1 of the Supporting Information; positive HRESIMS ion, *m*/*z* 197.0713 $[M + H]^+$ (calculated for $C_{12}H_9N_2O$, 197.0709).

*Hydroxyquinone (**4**):* Yellow, amorphous powder; UV (MeOH) λ_{max}, 210, 270, 390 nm; ^1H and ^{13}C NMR data, see Table S3 of the Supporting Information; negative HRESIMS ion, *m*/*z* 305.2126 $[M - H]^-$ (calculated for $C_{19}H_{29}O_3$, 305.2122).

*Furanone (**5**):* White, amorphous powder; UV (MeOH) λ_{max}, 200, 220, 280 nm; ^1H and ^{13}C NMR data, see Table 1 and Table S2 of the Supporting Information; negative HRESIMS ion, *m*/*z* 309.2073 $[M - H]^-$ (calculated for $C_{18}H_{29}O_4$, 309.2071).

*Furanone (**6**):* White, amorphous powder; UV (MeOH) λ_{max}, 200, 220, 280 nm; ^1H and ^{13}C NMR data, see Table 1 and Table S4 of the Supporting Information; positive HRESIMS ion, *m*/*z* 305.1720 $[M + Na]^+$ (calculated for $C_{16}H_{26}O_4Na$, 305.1723).

*Hydroxyquinone (**7**):* Yellow, amorphous powder; UV (MeOH) λ_{max}, 210, 270, 390 nm; ^1H and ^{13}C NMR data, see Table 2; negative HRESIMS ion, *m*/*z* 277.1814 $[M - H]^-$ (calculated for $C_{17}H_{25}O_3$, 277.1809).

*Dialkylresorcinol−Hydroxyquinone Dimer (**8**):* Red, amorphous powder; UV (MeOH) λ_{max}, 230, 275, 375, and 490 nm; ^1H and ^{13}C NMR data, see Table 2 and Table S5 of the Supporting Information; positive HRESIMS ion, *m*/*z* 541.3887 $[M - H]^-$ (calculated for $C_{34}H_{53}O_5$, 541.3888).

*Hydroxyquinone Dimer (**9**):* Yellow, amorphous powder; UV (MeOH) λ_{max}, 230, 280, 400 nm; ^1H and ^{13}C NMR data, see Table 2 and Table S6 of the Supporting Information; positive HRESIMS ion, *m*/*z* 553.3536 $[M - H]^-$ (calculated for $C_{34}H_{49}O_6$, 553.3535).

Antimicrobial Testing. For agar well diffusion assays, dried samples were dissolved in sterile water and dimethyl sulfoxide (DMSO, <5%) to make a sample solution with a concentration at 10 mg/mL. Appropriate antibiotics (2 mg/mL; see Table S7 of the Supporting Information) were used as the positive control, while sterile water with DMSO (<5%) was used as the negative control.

ATCC pathogens were suspended in sterile water until optical density at 585 nm reached 1.00 (±0.02) [cell density is about 10^8 colony-forming units (CFU)/mL]. A 200 μL pathogen suspension was spread on the appropriate solid media and let to stand for 10 min. Wells (5 mm) were then punched out of the media plates using a sterile pipet tip. Samples (30 μL) were added to the well. Plates were incubated for 12 h at the optimal growth temperature (see Table S7 of the Supporting Information), and inhibition zones were observed and measured. For MIC determination, a modified form of a literature protocol was used with appropriate antibiotics as the positive control and sterile water/DMSO (<5%) as the negative control (page S43 of the Supporting Information).[30]

■ ASSOCIATED CONTENT

Supporting Information

The Supporting Information is available free of charge at https://pubs.acs.org/doi/10.1021/acs.jnatprod.9b00315.

Tabulated NMR data for compounds **2**−**9**, including two-dimensional (2D) data for compounds **4**−**9**, details on antimicrobial test strains, $HRMS^2$ data for compounds **1**, **2**, **5**, **6**, **8**, and **9**, NMR and HRESIMS spectra for compounds **1**−**9**, and detailed protocols for microbe identification and antimicrobial tests (PDF)

■ AUTHOR INFORMATION

Corresponding Author

Benjamin R. Clark − *School of Pharmaceutical Science and Technology, Tianjin University, Tianjin 300072, People's*

https://dx.doi.org/10.1021/acs.jnatprod.9b00315
J. Nat. Prod. XXXX, XXX, XXX−XXX

Republic of China; orcid.org/0000-0001-8987-7092; Phone: +86-22-87401830; Email: bclark@tju.edu.cn

Authors

Yue Shi − *School of Pharmaceutical Science and Technology, Tianjin University, Tianjin 300072, People's Republic of China*

Diana A. Zaleta-Pinet − *School of Pharmaceutical Science and Technology, Tianjin University, Tianjin 300072, People's Republic of China*

Complete contact information is available at: https://pubs.acs.org/10.1021/acs.jnatprod.9b00315

Notes

The authors declare no competing financial interest.

■ ACKNOWLEDGMENTS

This work was funded in part by the award from the Research Fund for International Young Scientists (81850410550) from the National Science Foundation of China and a grant from the National Basic Research Program of China (2015CB856500). The authors acknowledge Y. Gao for assistance in acquisition of MS−MS data and Prof. J. De Voss for his helpful comments on the decomposition mechanism.

■ REFERENCES

(1) Bolivar, P.; Cruz-Paredes, C.; Hernández, L. R.; Juárez, Z. N.; Sánchez-Arreola, E.; Av-Gay, Y.; Bach, H. *J. Ethnopharmacol.* **2011**, *137*, 141−147.
(2) Koehn, F. E.; Carter, G. T. *Nat. Rev. Drug Discovery* **2005**, *4*, 206−220.
(3) Bachmann, B. O.; Van Lanen, S. G.; Baltz, R. H. *J. Ind. Microbiol. Biotechnol.* **2014**, *41*, 175−184.
(4) Patwardhan, B.; Warude, D.; Pushpangadan, P.; Bhatt, N. *Evid-Based. Compl. Alt.* **2005**, *2*, 465−473.
(5) Wang, Q.; Hu, Z. Q.; Li, X. X.; Wang, A. L.; Wu, H.; Liu, J.; Cao, S. G.; Liu, Q. S. *J. Nat. Prod.* **2018**, *81*, 2531−2538.
(6) Sun, N.; Zhu, Y.; Zhou, H. F.; Zhou, J. F.; Zhang, H. Q.; Zhang, M. K.; Zeng, H.; Yao, G. M. *J. Nat. Prod.* **2018**, *81*, 2673−2681.
(7) Wang, J. J.; Chen, F. M.; Liu, Y. H.; Liu, Y. X.; Li, K. L.; Yang, X. L.; Liu, S. W.; Zhou, X. F.; Yang, J. *J. Nat. Prod.* **2018**, *81*, 2722−2730.
(8) Yang, L.; Li, H. X.; Wu, P.; Mahal, A.; Xue, J. H.; Xu, L. X.; Wei, X. Y. *J. Nat. Prod.* **2018**, *81*, 1928−1936.
(9) Feklistova, I. N.; Maksimova, N. P. *Microbiology* **2008**, *77*, 176−180.
(10) Raaijmakers, J. M.; De Bruijn, I.; Nybroe, O.; Ongena, M. *FEMS Microbiol. Rev.* **2010**, *34*, 1037−1062.
(11) Bassarello, C.; Lazzaroni, S.; Bifulco, G.; Lo Cantore, P.; Iacobellis, N. S.; Riccio, R.; Gomez-Paloma, L.; Evidente, A. *J. Nat. Prod.* **2004**, *67*, 811−816.
(12) Mehnaz, S.; Saleem, R. S. Z.; Yameen, B.; Pianet, I.; Schnakenburg, G.; Pietraszkiewicz, H.; Valeriote, F.; Josten, M.; Sahl, H. G.; Franzblau, S. G.; Gross, H. *J. Nat. Prod.* **2013**, *76*, 135−141.
(13) Sharma, A.; Jansen, R.; Nimtz, M.; Johri, B. N.; Wray, V. *J. Nat. Prod.* **2007**, *70*, 941−947.
(14) Pohanka, A.; Broberg, A.; Johansson, M.; Kenne, L.; Levenfors, J. *J. Nat. Prod.* **2005**, *68*, 1380−1385.
(15) Pohanka, A.; Levenfors, J.; Broberg, A. *J. Nat. Prod.* **2006**, *69*, 654−657.
(16) Kanda, N.; Ishizaki, N.; Inoue, N.; Oshima, M.; Handa, A.; Kitahara, T. *J. Antibiot.* **1975**, *28*, 935−942.
(17) Kato, S.; Shindo, K.; Kawai, H.; Matsuoka, M.; Mochizuki, J. *J. Antibiot.* **1993**, *46*, 1024−1026.
(18) Stodola, F. H.; Weisleder, D.; Vesonder, R. F. *Phytochemistry* **1973**, *12*, 1797−1798.
(19) Beresovsky, D.; Hadas, A.; Livne, O.; Sukenik, A.; Kaplan, A.; Carmeli, S. *Isr. J. Chem.* **2006**, *46*, 79−87.
(20) Imai, S.; Fujioka, K.; Furihata, K.; Furihata, K.; Seto, H. *J. Antibiot.* **1993**, *46*, 1323−1325.
(21) Nowak-Thompson, B.; Hammer, P. E.; Hill, D. S.; Stafford, J.; Torkewitz, N.; Gaffney, T. D.; Lam, S. T.; Molnár, I.; Ligon, J. M. *J. Bacteriol.* **2003**, *185*, 860−869.
(22) Kolbert, C. P.; Persing, D. H. *Curr. Opin. Microbiol.* **1999**, *2*, 299−305.
(23) Singh, U. S.; Scannell, R. T.; An, H.; Carter, B. J.; Hecht, S. M. *J. Am. Chem. Soc.* **1995**, *117*, 12691−12699.
(24) Philipp, B.; Schink, B. *J. Bacteriol.* **1998**, *180*, 3644−3649.
(25) Akee, R. K.; Ransom, T.; Ratnayake, R.; McMahon, J. B.; Beutler, J. A. *J. Nat. Prod.* **2012**, *75*, 459−463.
(26) Clark, B. R.; Capon, R. J.; Lacey, E.; Tennant, S.; Gill, J. H. *Org. Biomol. Chem.* **2006**, *4*, 1520−1528.
(27) Clark, B. R.; Capon, R. J.; Lacey, E.; Tennant, S.; Gill, J. H. *Org. Biomol. Chem.* **2006**, *4*, 1512−1519.
(28) Scott, A. I. *Interpretation of the Ultraviolet Spectra of Natural Products*; Pergamon Press: Oxford, U.K., 1964; pp 95−96.
(29) Brameyer, S.; Kresovic, D.; Bode, H. B.; Heermann, R. *Proc. Natl. Acad. Sci. U. S. A.* **2015**, *112*, 572−577.
(30) Wayne, P. A. *Methods for Dilution Antimicrobial Susceptibility Tests for Bacteria That Grow Aerobically: Approved Standard*; Clinical and Laboratory Standards Institute (CLSI): Wayne, PA, 2015.